JOURNAL OF GEOPHYSICAL RESEARCH, VOL. 107, NO. D24, 4798, doi:10.1029/2001JD002037, 2002

Interannual variability of the 4-day wave and isentropic mixing inside the polar vortex in midwinter of the Southern Hemisphere upper stratosphere

Ryo Mizuta and Shigeo Yoden
Department of Geophysics, Kyoto University, Kyoto, Japan

Received 26 December 2001; revised 18 April 2002; accepted 23 April 2002; published 28 December 2002.

[1] Interannual variations of the flow field and large-scale horizontal transport and mixing inside the wintertime polar vortex of the Southern Hemisphere upper stratosphere are investigated using isentropic winds obtained from the U.K. Met Office assimilated data for nine years of 1992–2000. We focused on the midwinter, July, when the polar vortex is not much distorted, although an eastward propagating wave called the 4-day wave is observed in some years in the polar region. Finite-time Lyapunov exponents are computed, and contour advections are done to examine stirring and mixing in the polar region. When the 4-day wave has a large amplitude, effective mixing through a stretching and folding process is seen inside the polar vortex. Finite-time Lyapunov exponents are sometimes as large as the midlatitudes, and the material contours of small areas grow exponentially in time on the poleward side of 70°S. Such mixing properties are not uniform inside the vortex. When the wave is not clearly seen, on the other hand, wind fields are close to a solid body rotation around the pole, and mixing is very small; Lyapunov exponents are small, and the material contours grow linearly in time by the stretching due to the meridional shear of the polar night jet. Such interannual variability of the strength of the mixing is correlated with the variability of the perturbation amplitude of potential vorticity in the polar region. *INDEX TERMS:* 0341 Atmospheric Composition and Structure: Middle atmosphere—constituent transport and chemistry (3334); 3334 Meteorology and Atmospheric Dynamics: Middle atmosphere dynamics (0341, 0342); 3220 Mathematical Geophysics: Nonlinear dynamics;
KEYWORDS: stratosphere, mixing, variability

Citation: Mizuta, R., and S. Yoden, Interannual variability of the 4-day wave and isentropic mixing inside the polar vortex in midwinter of the Southern Hemisphere upper stratosphere, *J. Geophys. Res.*, *107*(D24), 4798, doi:10.1029/2001JD002037, 2002.

1. Introduction

[2] The winter stratosphere can be separated into three regions from the viewpoint of transport and mixing; the polar region, midlatitudes, and the tropics [e.g., *Holton et al.*, 1995; *Haynes and Shuckburgh*, 2000]. There is slow upwelling in the tropics and downwelling in the polar region due to wave drags. These three regions can be distinguishable in the global-scale distributions of chemical tracers since transport barriers exist between these regions to suppress the horizontal transport through the boundaries [e.g., *Plumb*, 2002]. Tracers are well mixed in the midlatitudes, called as the "surf zone," due to Rossby-wave breaking. The barrier dividing the polar region and midlatitudes is the polar vortex edge, associated with a large horizontal gradient of potential vorticity (PV). The position of the barrier between the midlatitudes and the tropics is less evident than that between the polar region and midlatitudes.

[3] Mixing in the polar region, or inside the polar vortex, in midwinter is generally thought to be much less than in the "surf zone" according to the studies of the mixing inside the vortex, many of which are focused on the middle or lower stratosphere. *Schoeberl et al.* [1992] found eddy mixing rates in the vortex to be an order of magnitude less than those in the midlatitudes. Similar results are shown in the advection calculation of many particles on an isentropic surface [*Bowman*, 1993] and the advection calculation of material contours [*Norton*, 1994], except that there is strong stirring inside the vortex when the polar vortex is highly distorted by large-amplitude wave events in the Northern Hemisphere [*Plumb et al.*, 1994; *Pierce et al.*, 1994]. These studies are based on the results of advections on particular isentropic surfaces, while effective diffusivity below 850 K isentropic surface examined by *Haynes and Shuckburgh* [2000] shows small mixing almost everywhere inside the polar vortex below 850 K surface, except above 700 K surface in the midwinter in the Southern Hemisphere. The smaller mixing rate seems to be generally the case as a climatology of the polar vortex of the lower stratosphere in the Southern Hemisphere winter [*Allen and Nakamura*, 2001].

[4] In our previous model study [*Mizuta and Yoden*, 2001], we used a two-dimensional nondivergent model to

0148-0227/02/2001JD002037$09.00

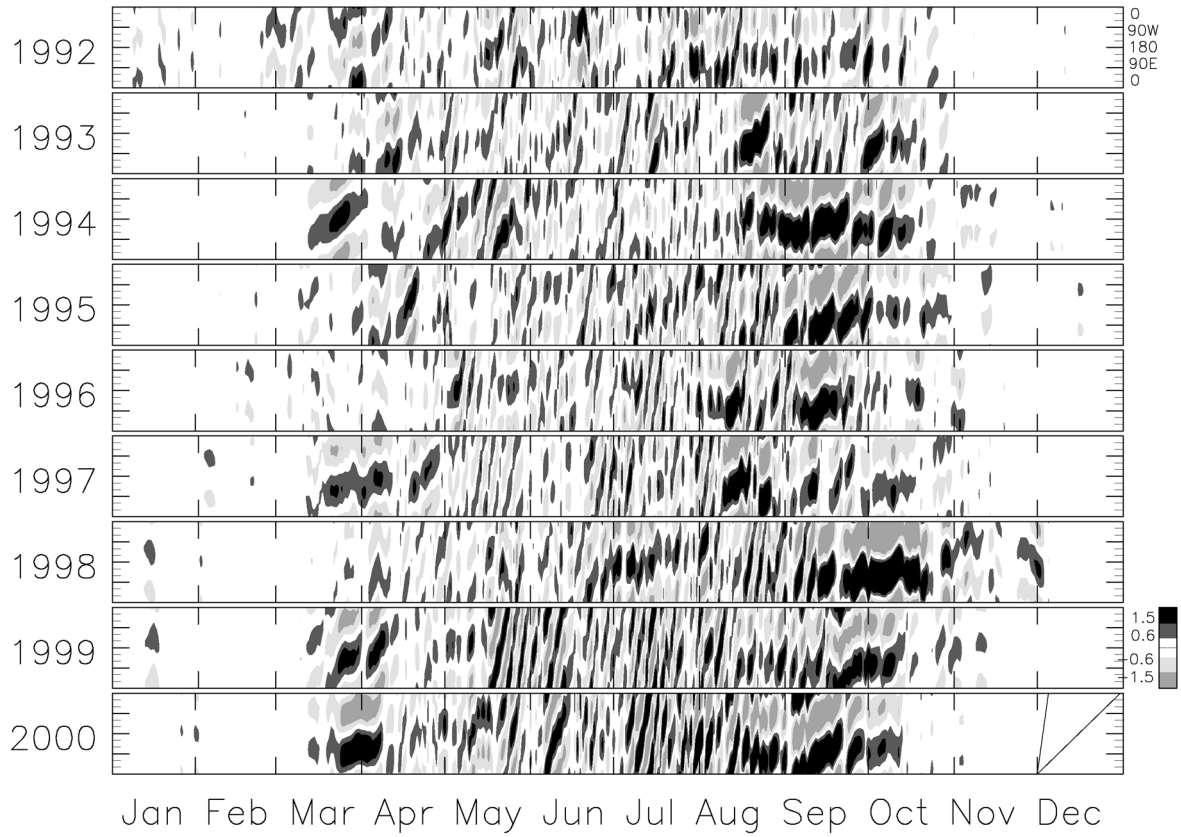

Figure 1. Time-longitude sections of the wavenumber 1 component of PV along 72°S on 1800 K isentropic surface (approximately 1hPa). 1 unit represents 10^{-3} Km^2s^{-1} kg^{-1}. The lines of constant phase in the section of Dec 2000 are those for the periods of 4 days and 30 days.

simulate quasi-periodic behavior of the polar vortex by giving a westerly jet forcing. The spatial patterns obtained in particle advections were very complicated inside the polar vortex, although the flow field was relatively simple. The quasi-periodicity was intended to mimic the behavior of the 4-day wave that appears in the wintertime upper stratosphere [*Venne and Stanford*, 1979], more evidently in the Southern Hemisphere than in the Northern Hemisphere. It is dominated by zonal wavenumbers from 1 to 4, traveling eastward with the same phase speed. Observational and theoretical studies on the 4-day wave are summarized by *Allen et al.* [1997] and *Manney et al.* [1998]. *Hartmann* [1983] examined linear stability of an idealized polar night jet and pointed out that the barotropic instability of a zonally symmetric jet profile can cause the 4-day wave. *Manney et al.* [1988] investigated the barotropic instability of observed jet profiles in the Southern Hemisphere winter and found good agreement with the characteristics of the observed wave. A three-dimensional model study by *Manney and Randel* [1993] showed that both barotropic and baroclinic instability play an important role in 4-day wave amplification.

[5] In this study, assimilated data for nine years are used to investigate mixing processes in midwinter on an isentropic surface in the Southern Hemisphere upper stratosphere, in which the situation of the flow field is close to that in the model study by *Mizuta and Yoden* [2001]. The interannual variation of the flow is related to the barotropic and baroclinic instability of the polar night jet. Since the amplitudes of the planetary waves propagating upward from the troposphere are small in midwinter in the Southern Hemisphere, the polar vortex keeps its shape without large distortions, and the mixing is not affected by the transport across the polar vortex edge. We focus on the interannual variability of the strength of the mixing inside the polar vortex, and study how the mixing is related to the disturbances of the flow field.

[6] Brief description about the data is given in section 2. In section 3, the interannual variability of the flow field is described, and comparison of the mixing inside the polar vortex between two characteristic years, and the relationship of the mixing with the flow for all the years are shown in section 4. Discussion is in section 5, and section 6 is the conclusions.

2. Data

[7] The United Kingdom Meteorological Office assimilated data [*Swinbank and O'Neill*, 1994] of nine years (1992–2000) are used for advection experiments on isentropic surfaces. The daily global data are available on a $2.5° \times 3.75°$ latitude-longitude grid at 22 pressure levels ranging from 1000 to 0.3 hPa. *Manney et al.* [1998] compared the transport calculations using the Met Office wind data and the satellite observations of H_2O and CH_4,

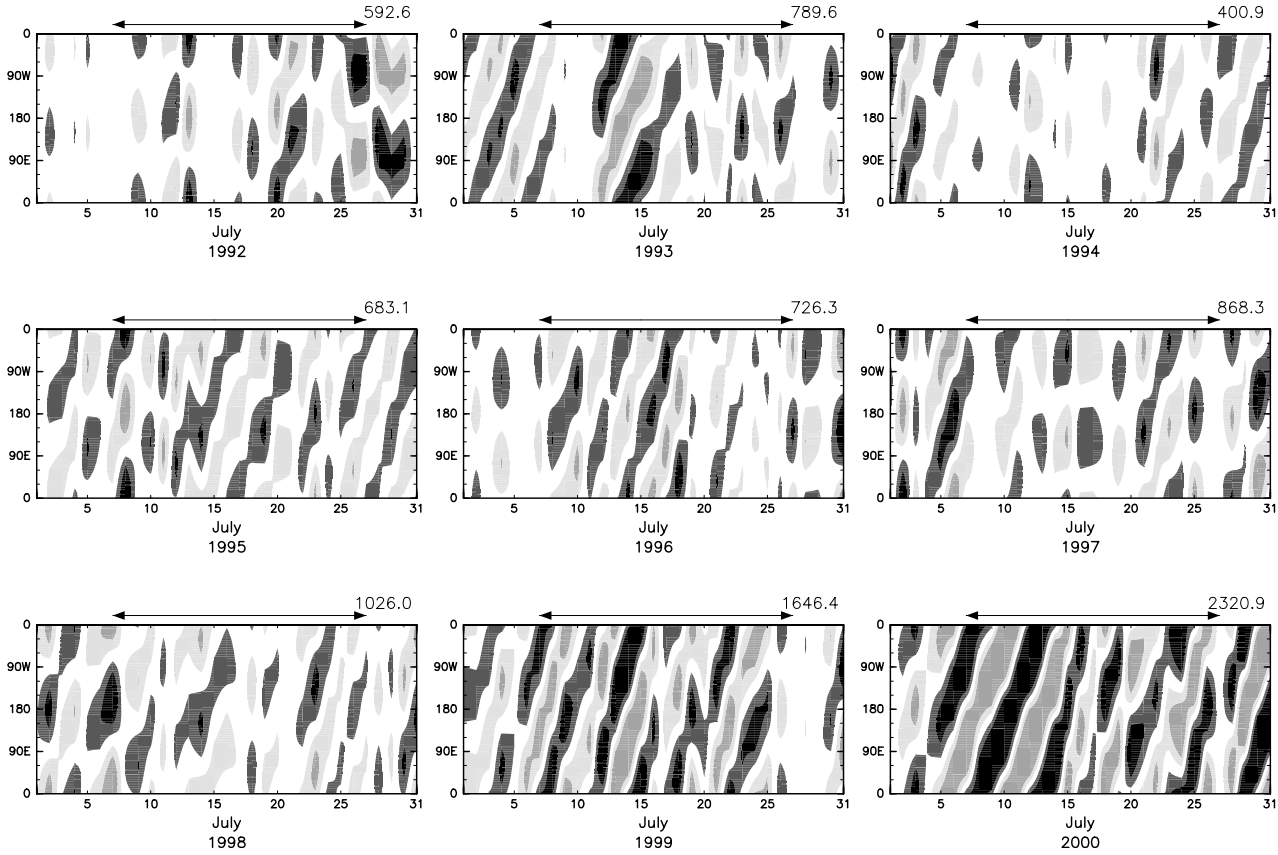

Figure 2. Time-longitude sections of the wavenumber 1 component in PV along 72°S on 1800 K surface in July, showing fast-moving component by substracting 7-day running mean. Arrows denote the duration of the advection calculation (July 7 to 27), and the values above each panel are the avarage of $\overline{q'^2}$ during that time.

and showed that the data in the upper polar stratosphere in winter are generally reliable for transport calculations.

[8] Horizontal wind data are interpolated in the vertical onto isentropic surfaces, and linearly interpolated in time. The data on isentropic surfaces are expanded to spherical harmonics and wind velocities on any arbitrary points are calculated by inverse transformation of the spectrum. Particle advections, contour advections, and finite-time Lyapunov exponents are calculated with the obtained wind velocities by using the same algorithm described by *Mizuta and Yoden* [2001].

3. Interannual Variations of the Flow Field

3.1. Hovmöller Diagrams

[9] Figure 1 shows time-longitude sections of the zonal wavenumber 1 component in PV along 72°S on 1800 K isentropic surface (approximately 1 hPa level). Wave disturbances are seen in three seasons except for summer, and the amplitude of the wavenumber 1 is larger than the other wave components all through the seasons. Three types of the wave are identified in the diagrams, that is, a stationary wave, a slow eastward propagating wave with a period of a few weeks, and a fast eastward propagating wave with a period of several days. The stationary wave is dominant in September and October until the breakdown of the polar vortex. The phase is almost fixed positive in the eastern hemisphere, and negative in the western hemisphere [*Harwood*, 1975]. The slow eastward propagating wave is seen rather occasionally in March, April and August. Its details are analyzed by *Hsu and Weng* [2002]. The fast wave is frequently seen from May through August, some of which is overlayed with the slow wave as in May of 1994.

[10] Fast propagating components of the diagrams in July are shown in Figure 2, by subtracting 7-day running mean. The eastward propagating wave with a period of about 4 days corresponds to the 4-day wave referred in the introduction. There is considerable interannual variability in the amplitude of the wave. The variability is not only in the amplitude but in the duration, height and latitude of its appearance. As long as we can see on this height and latitude, however, the amplitude of the wave is large all through the month in 1998, 1999, and particularly in 2000, while it is very small in 1992 and 1994. These are quantified by the values above each panel of Figure 2, which denote the average of $\overline{q'^2}$ during the 20 days displayed by arrows (July 7 to 27), where an overbar denotes the zonal mean and q' is the PV deviation from the zonal mean.

3.2. Zonal Mean Profiles

[11] Zonal mean profiles of zonal wind $\overline{u}$ and PV $\overline{q}$ on 1800 K isentropic surface for these nine years are shown in

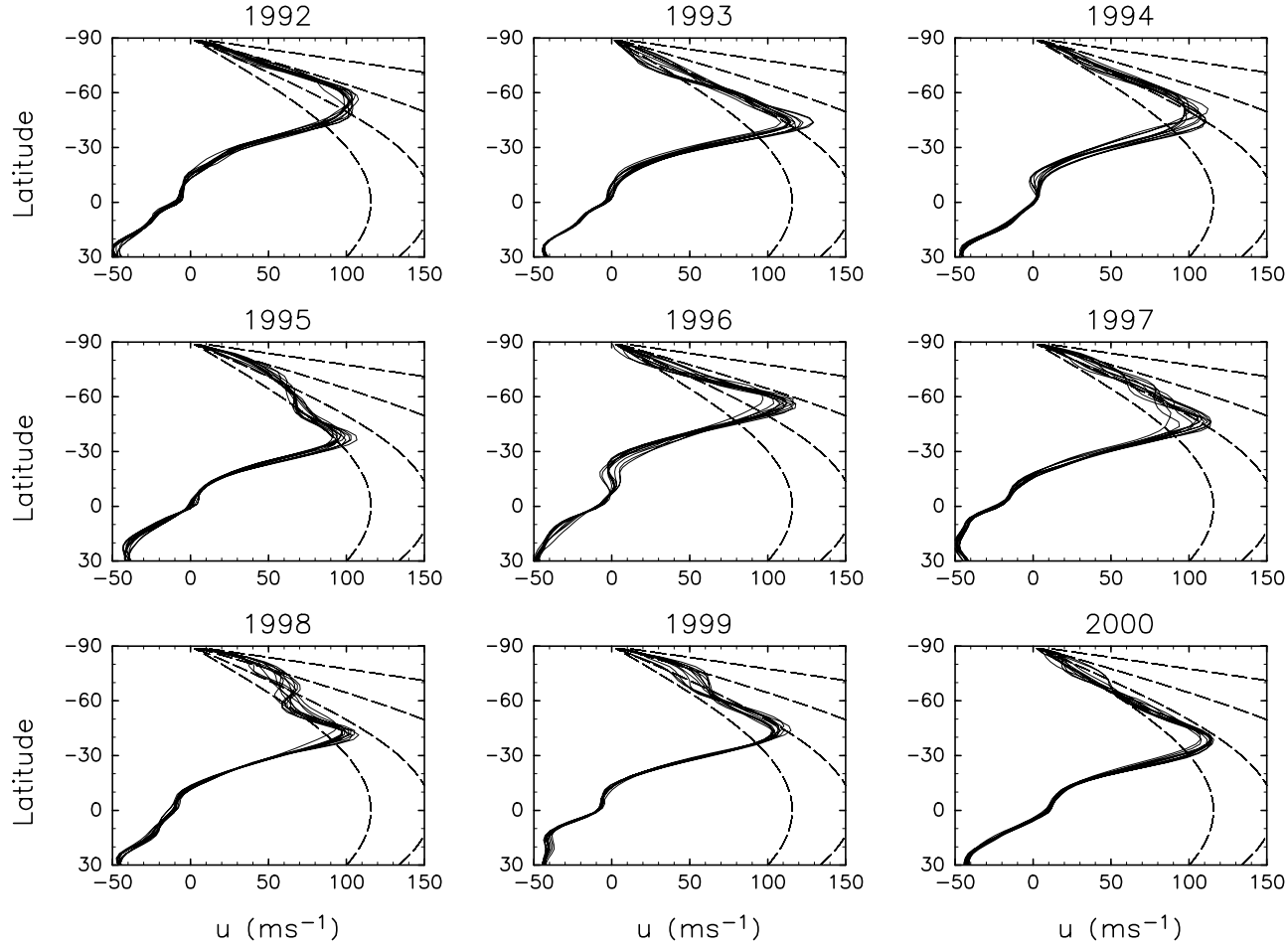

Figure 3. Zonal mean profiles of zonal wind $\overline{u}$ as a function of latitude on 1800 K isentropic surface. The profiles at each of 10 days from July 7 are drawn. Dashed lines are the velocities equivalent to the solid body rotation with the period from 1 to 4 days.

Figures 3 and 4, respectively. The profiles for each of 10 days from July 7 are drawn. The location of the polar vortex edge, judged from the maximum wind speed in Figure 3 and the maximum gradient of PV in Figure 4, is not very different for each 10 days, but has large interannual variability from 40°S to 60°S. The location is more equatorward side than that in the lower stratosphere.

[12] The meridional profiles of PV inside the polar vortex show monotonic increase with latitude in some years as 1992, 1994, and 1997, while they have opposite gradients in other years as 1993, 1998, 1999, and 2000. A linear stability criterion shows the zonal mean zonal flow itself is not dynamically unstable with monotonically varying PV. In the years with monotonically varying PV, the profiles of $\overline{u}$ in the polar region are close to the solid body rotation with the period of 2 or 3 days, which are denoted by dashed lines in Figure 3 together with those for the period of 1 or 4 days. If PV has a counter gradient, on the other hand, the flow can be barotropically unstable and perturbations are expected to grow to have a finite amplitude. The eastward propagating wave in Figure 2 is thought to be excited by the instability mechanism [e.g., *Allen et al.*, 1997]. However, the counter gradient of PV is not very clear in some of the years when eastward propagating wave is evident. Note that the wave is roughly stationary with respect to the zonal mean zonal flow since the flow speed of these years are such that air parcels go round the pole in 3 or 4 days.

3.3. Time Evolution of PV

[13] We compare two extreme years of 1994 and 2000, in which the amplitude of the 4-day wave is smallest or largest in all the available data. Calculations of PV field on 1800 K isentropic surface are done for 20 days starting at July 7, during which the wave amplitude is largest in 2000. The same period in 1994 is investigated to avoid the influence of the seasonal march.

[14] The evolutions of PV field in 2000 and 1994 are shown in Figures 5 and 6, respectively. The thick line is the vortex edge defined as the isoline of PV where the gradient of PV is largest in the equivalent-latitude coordinate. A couple of regions of relatively high anti-cyclonic PV, which is as high as that on the polar vortex edge, are seen inside the vortex in 2000. As denoted by the arrow in Figure 5, they move eastward with the speed of about 90 degrees per day in the latitude from 60°S to 80°S, the speed of which is comparable to the background westerly wind. These structures correspond to the eastward propagating waves in Figure 2. Variation of the shape of the polar vortex is not

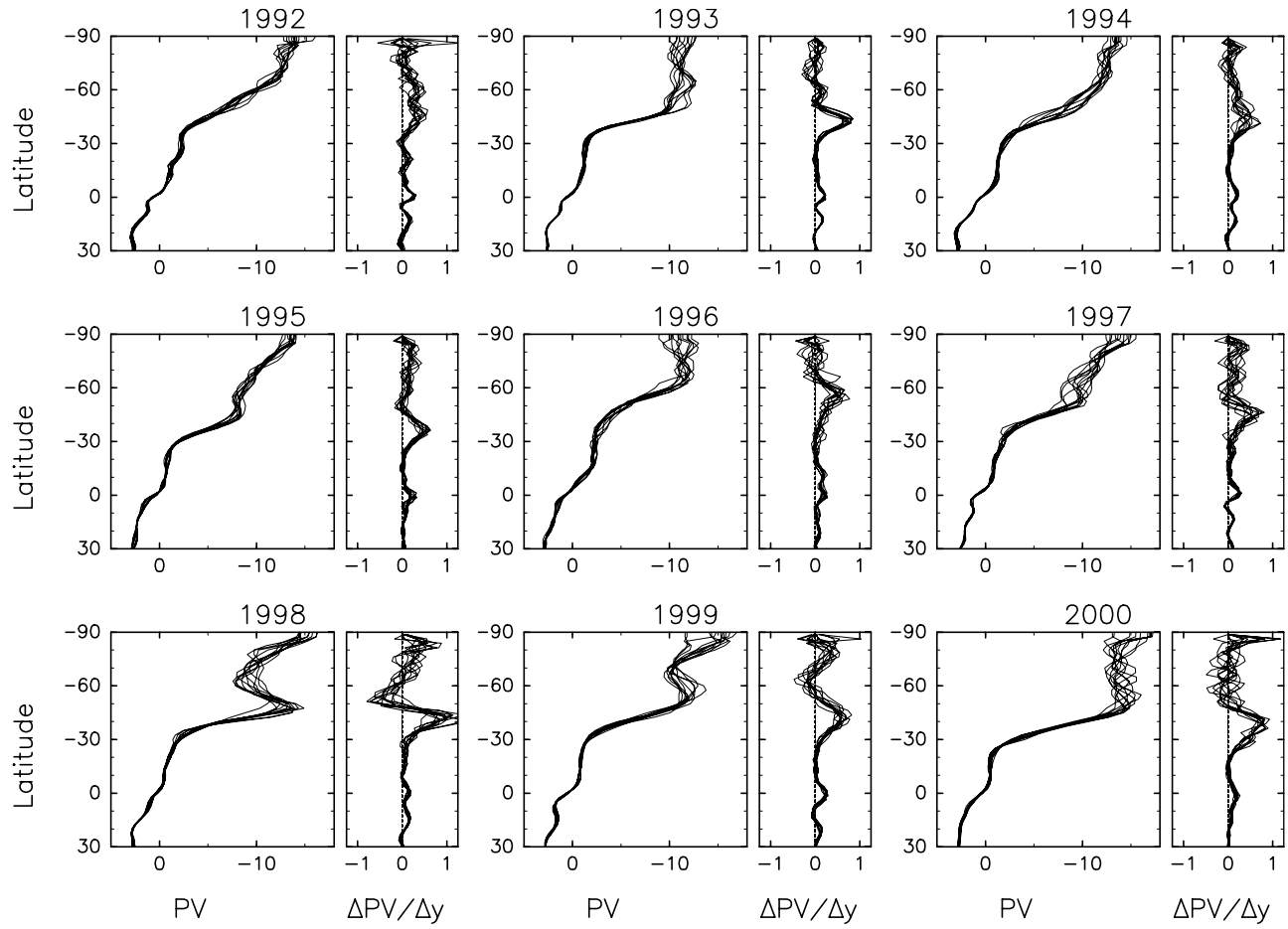

Figure 4. Zonal mean profiles of PV $\overline{q}$ and its meridional gradient as a function of latitude on 1800 K isentropic surface. Profiles at each of 10 days from July 7 are drawn. 1 unit for the PV is 10^{-3} Km^2s^{-1} kg^{-1}. 1 unit for the gradient is 10^{-5} Kms^{-1} kg^{-1}.

very evident and any typical wave-breaking pattern is not found. Such an isolated structure of relatively high PV is not seen in 1994 on this height and period. The area inside the polar vortex is smaller than that in 2000. A small wave-breaking pattern is seen on July 15 and 16.

4. Interannual Variation of the Isentropic Mixing Properties

4.1. Particle Advection

[15] Many particles are initially placed on concentric circles centered on the south pole with 5° latitude intervals from 30°S to 85°S, and their longitudinal interval is approximately 10 km. Advections of these particles are calculated for 20 days starting at July 7. Only the particles initially inside the polar vortex are shown in Figures 7 and 8, although strong stirring always occurs outside the polar vortex. As shown in many previous studies, transport between both sides of the vortex edge is very little, judging from the fact that the region where the particles exist after 10 days and the region defined to be inside of the vortex at that time are almost identical. Small amount of ejection and intrusion across the vortex edge is seen after 20 days in 2000 and 1994, respectively, although the accuracy of total divergence or convergence within the polar vortex needs to be certified.

[16] Here we pay attention to the inside of the vortex. Each chain of particles can be regarded as an material line as far as their dispersion is small. A shape of tongue similar to a wave-breaking pattern is formed on poleward side of 70°S after 3 days in 2000 as shown in Figure 7. Materials on the poleward side of 60°S are continuously stirred by forming such patterns. Although PV fields are limited in resolution and quality, it should be noted that PV fields in Figure 5 do not show such patterns owing to non-conservative nature of PV in the region. A fairly large mixing takes place in this region in 20 days, through the enhancement of the efficiency of small-scale mixing by increasing the interfacial contour length. By contrast, there is very little mixing on equatorward side of 60°S even after 20 days advection; material lines are still discernible. In 1994, however, each chain of particles can be discernible after 10 days all inside the polar vortex as shown in Figure 8. Polar region does not experience much distortion even after 20 days. Material lines are stretched near 60°S, but only in the zonal direction.

4.2. Contour Advection

[17] In order to examine how nearby particles spread with time, free from the meridional and zonal directions, material contours are initially put along small circles with a radius of

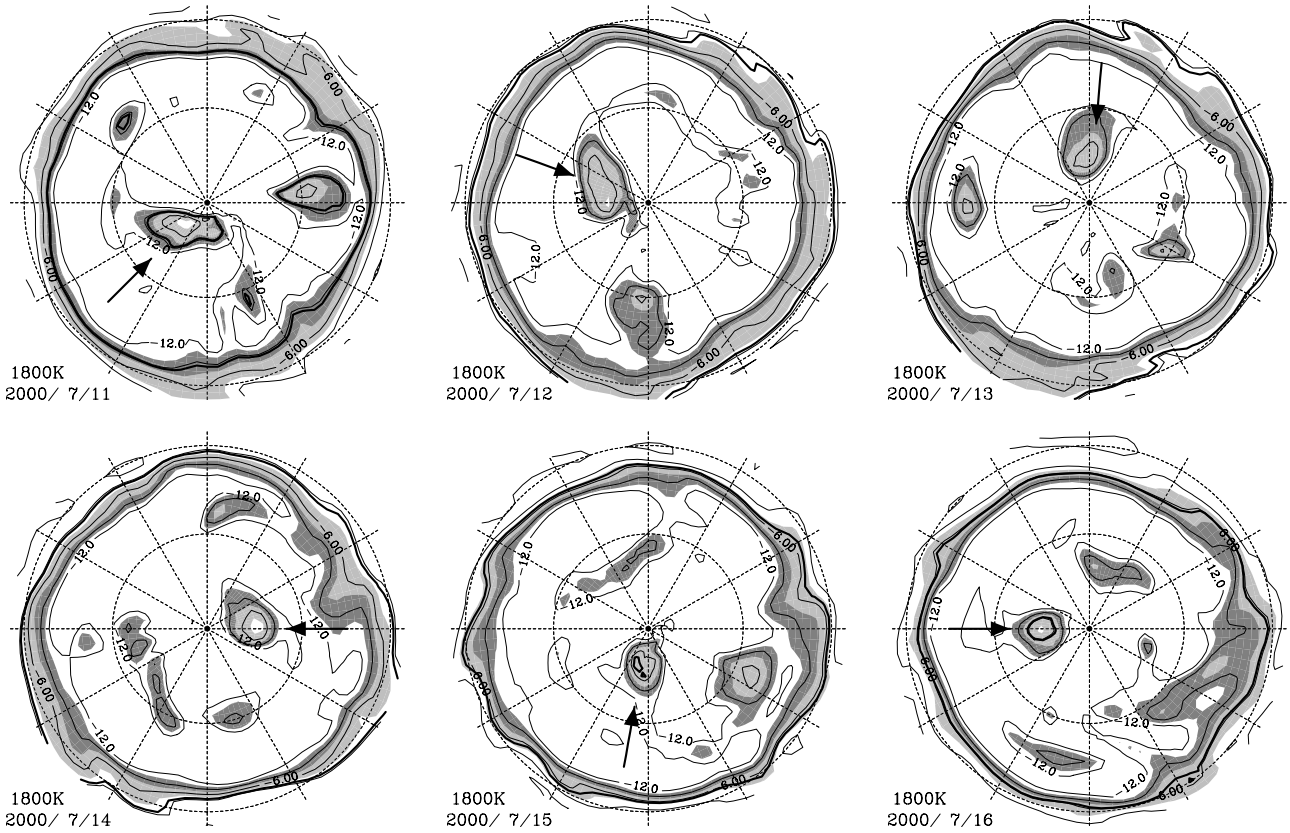

Figure 5. Time evolution of PV field on 1800 K isentropic surface in 2000. The maps are Lambert equal area projections, with the dashed lines of 30°S and 60°S latitude circles. Thick lines are the polar vortex edge defined as the isoline of PV where the gradient of PV is largest in the equivalent latitude coordinate. 1 unit represents 10^{-3} Km^2s^{-1} kg^{-1}. Light-shaded is the region of PV from 4.5 to 7.5, and heavy-shaded is from 7.5 to 10.5.

0.05 rad and advections of the contours are calculated using contour advection technique [*Dritschel*, 1989; *Waugh and Plumb*, 1994]. Advections of the contours are examined by calculating trajectories of the points on the contours. The points are redistributed once a day so that the density of the distributed points depends on the curvature of the contours. A surgery algorithm that disconnects and reconnects contours is not included in this study. The circles are centered on grid points along major grid lines (as shown in Figure 11). The longest three contours and the shortest three ones after the 20-day advection in the two years are shown in Figure 9.

[18] Although the growth rate of the contour length inside the vortex is smaller than the outside (not shown), the longest three contours are stretched out to a thin line element in a short time in 2000. After the stretching, the element is distorted and folded. Stretching and folding processes are repeated and air parcels are mixed with surrounding. However, the inside of the polar vortex is not uniform and mixing is not so strong in some places. Well-mixed region is limited on poleward side of 60°S, and the parcels in the other region such as the shortest three contours keep their identities even after 20-day advection.

[19] In the case of 1994, on the other hand, stretching of the small circles is very small near the center of the vortex, suggesting that the parcels rotate around the pole like a rigid body. The longest contours are initially near the edge of the vortex. They are stretched only in the zonal direction by the meridional shear of the polar night jet, and slowly advected poleward by the convergence motion as mentioned in section 4.1.

4.3. Finite-Time Lyapunov Exponents

[20] As described above, the horizontal mixing inside the polar vortex is quite different qualitatively between the two years. Thus, we examine such interannual variability of the horizontal mixing for nine years available from the data.

[21] First, finite-time Lyapunov exponents are used as a quantitative measure of the two-dimensional stretching rate of air parcels. The largest exponent of the two gives the exponential growth rate of the distance between two nearby trajectories, depending on initial position and evaluation time. The numerical method used here is the same as that given by *Mizuta and Yoden* [2001], in which the evolutions of two orthonormal small perturbations are calculated after renormalizing the perturbations every one day.

[22] Figure 10 is the spatial distributions of the finite-time Lyapunov exponents with the evaluation time of 20 days starting at July 7 of each year of 1992–2000. The exponent is relatively large outside the polar vortex, suggesting that air parcels outside the vortex are always stirred and mixed strongly. Distinctive changes of the exponent is seen across

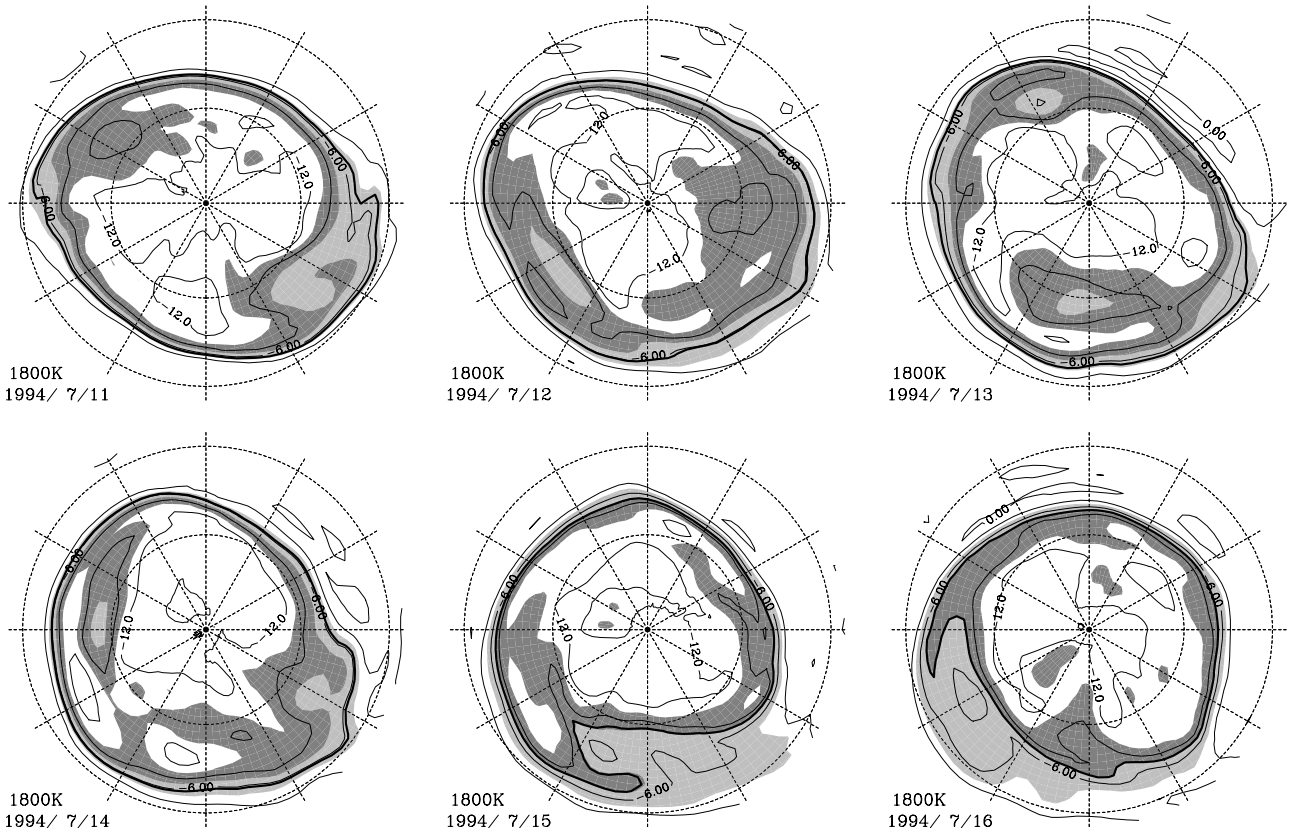

Figure 6. As in Figure 5, but in 1994.

the edge of the vortex, or the transport barrier, especially in 1993, 1996 and 1999. Inside the polar vortex, almost whole region is covered with small values of the exponent in 1992 and 1994. But it is not very uniform in the other years; in most cases, the exponent is relatively high around 70°S and lower around 50°S. In 1995, 1999, and 2000, the value around 70°S is as high as the outside. As an exceptional case, high exponent is observed in the whole region inside the vortex in 1998.

4.4. Length of the Contour

[23] The contour advection of initially small circles as shown in Figure 9 is calculated for all the nine years. The initial contours are put on the circles centered on the major latitude (every 5°) lines. Advections are calculated for 20 days starting at July 7, and the length of each contour after 20 days is shown with gray scale in Figure 11. Circles which existed outside the polar vortex at the initial time are not shown. Generally, the results are similar to the finite-time Lyapunov exponents, although the present measure reflects the nonlinear nature of advection. Contours near the pole are hardly stretched in 1992 and 1994, while those are stretched in the other years depending on the initial position.

[24] Time evolutions of the length of the contours relative to the initial length are shown in Figure 12. Contours initially put between 70°S and 85°S in Figure 11 are plotted in this figure, since contours in these latitudes are always defined to be inside the vortex. Thick lines denote the mean length of all these contours, and are fitted to the thick straight lines to obtain the exponential growth rate. Length of some contours can decrease with time, since some part of the contours is aligned to stretching directions and other part are to shrinking directions in the deformation field. Growth of the contours is basically exponential against time in 1995, 1999, and 2000. Almost all the individual contours in 2000 grow exponentially, while small part of the contours do not in 1995 and 1999. By contrast, any contours do not show such exponential growth in 1992 and 1994. In years such as 1996, the growth rate changes largely with time during the 20 days. This is due to the flow itself changing largely with time. The growth of the mean contour length is plotted for the nine years in Figure 13 in a logarithm scale (left) and in a linear scale (right). The growth in the latter half of the period seems to be categorized in two groups; in the years of 1995, 1998, 1999, and 2000, the mean contour length grows exponentially against time, while in the other years, growth of the mean length is close to a linear development, consistent with Figure 9 that material contours are stretched only by the horizontal shear near the polar night jet.

4.5. Correlation Between Wave Disturbance and Measures of Mixing

[25] All of the analyses described above show large interannual variability both in the flow field and the strength of the mixing inside the polar vortex. Relationships between them are examined for the nine years. Two quantities are used to characterize the strength of the disturbance in the polar region; mean $\overline{q'^2}$ for 20 days between 70°S and 85°S, and that for zonal wavenumber 1 component. On the other

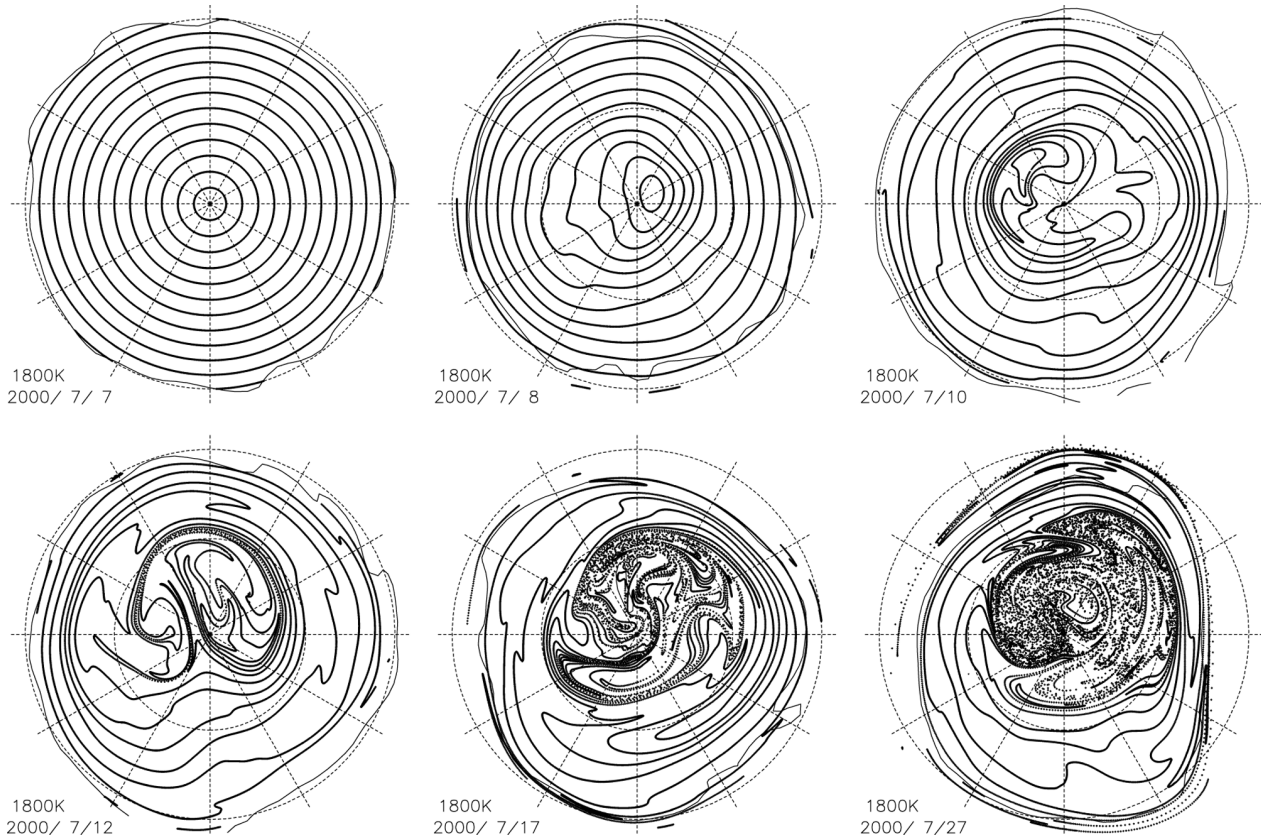

Figure 7. Advection of fluid particles for 20 days in 2000. Thin lines denote the vortex edge defined in Figure 5.

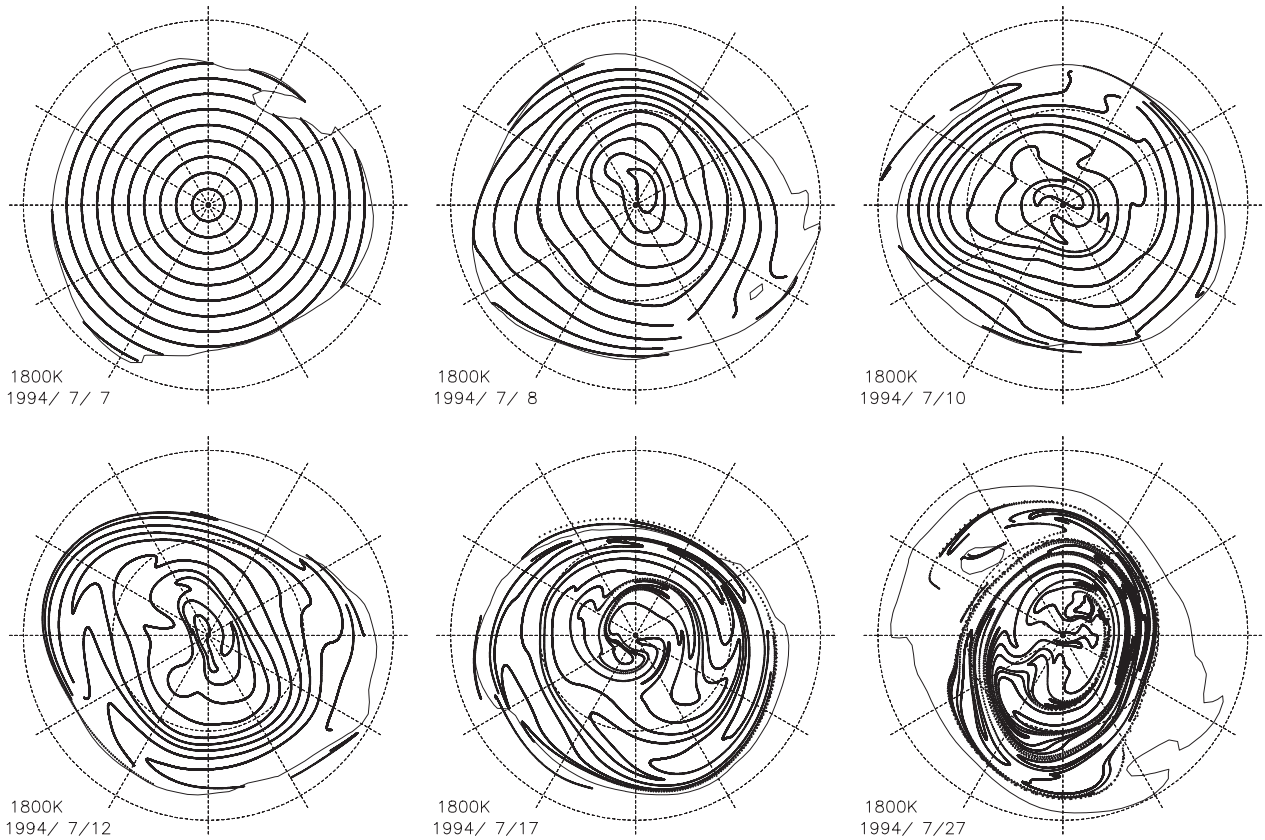

Figure 8. As in Figure 7, but in 1994.

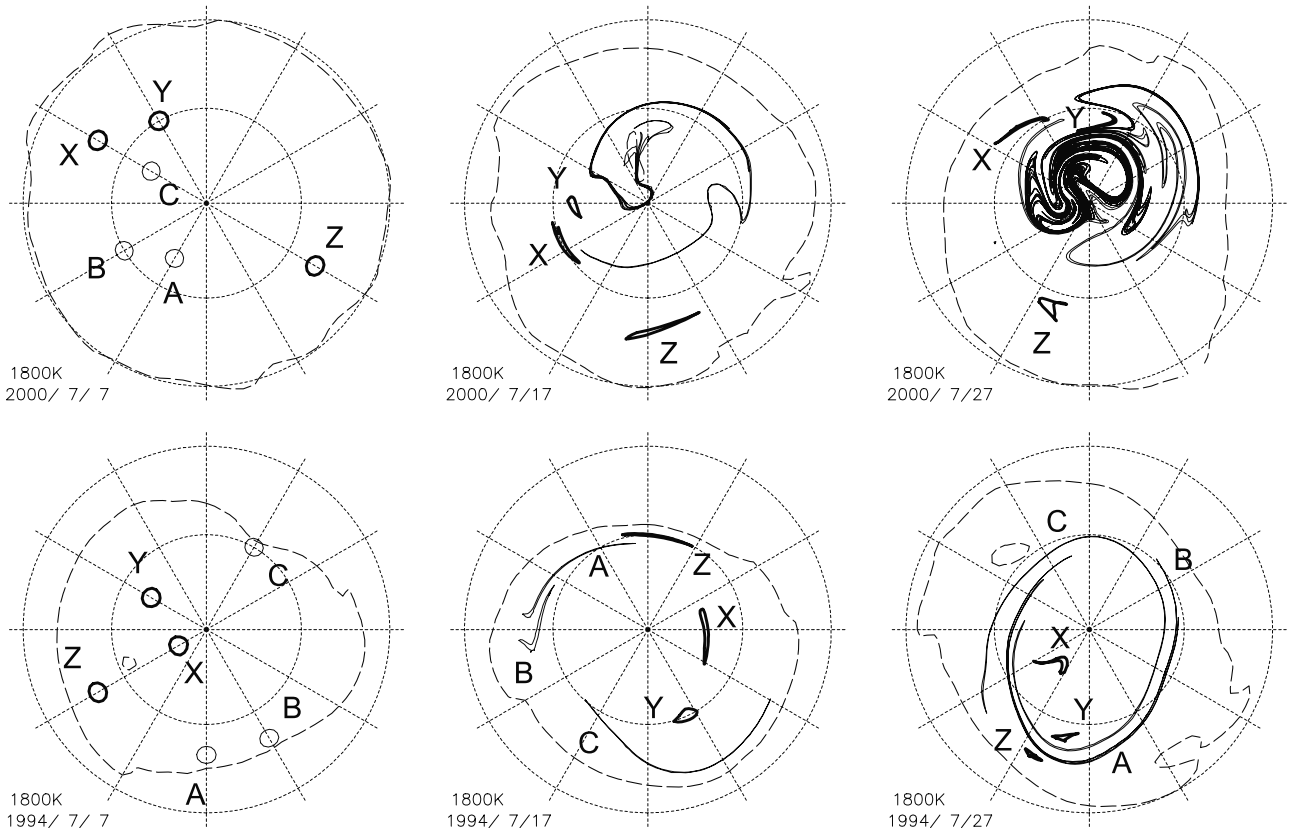

Figure 9. Advections of the six material contours. Thin contours (ABC) are the three longest ones after the 20-day advection. Thick contours (XYZ) are the three shortest ones. Initial positions of all the contours are shown in Figure 11.

hand, three quantities are used as representatives of the strength of the mixing; mean Lyapunov exponent between 70°S and 85°S in Figure 10, mean contour length after the 20-day advection in Figure 11, and mean growth rate of the contour in Figure 12. Relationships between these quantities for the nine years are shown in Figure 14, together with the correlation coefficients. We can see the tendency that the higher Lyapunov exponent corresponds to the larger perturbation amplitude, although the correlation coefficient is not so high as the others. The mean contour length after 20-day advection has the highest correlation coefficients over 0.9 with the disturbance amplitudes of both all waves and wavenumber 1, even though the available data are only nine years. The mean stretching rate is also well correlated to the disturbance amplitudes.

5. Discussion

[26] Interannual variability of the strength of the mixing and the amplitude of the disturbance in July show a good relationship in the polar region. Here we discuss how the hordizontal flow field is related to these characteristics. As shown in Figure 4, the latitudinal profile of the zonal mean PV shows monotonic increase inside the polar vortex in 1992, 1994, and 1997, while counter gradients in zonal mean PV exist inside the vortex in 1993, 1998, 1999, and 2000. In the former years, the flows are expected to be dynamically stable, and are close to a solid body rotation inside the vortex (Figure 3). As a result, the amplitude of the 4-day wave is small as shown in Figure 2. Therefore, the horizontal mixing in the polar region is also small as expected. By contrast, the counter gradient in the zonal mean PV in the latter years suggests that the zonal mean wind fields are barotropically unstable. It is expected that air parcels are stirred and well mixed by the perturbations growing through the instability. These expectations are certified in the results in 1999 and 2000, in which the amplitude of the eastward propagating wave is large and the mixing is strong. However, the correspondence is not always good; in 1998, the eastward propagating wave is not observed clearly in Figure 2 in spite of the large counter gradient in PV in midlatitudes, while the wave is clear in 1995 with little counter gradient in PV. The strength of the mixing shown in Figure 14 is comparable for these two years. Therefore, it is not highly related to the zonal mean flow field of the region. Development of the wave can be influenced by the flow field of different latitude, altitude, or time. The 4-day wave can develop through baroclinic instability, which is pointed out by *Manney and Randel* [1993]. It takes several days from the formation of the instability condition until the development of the disturbance. Therefore, it is necessary to extend the analysis to vertical structure and time development of the wind field as well as meridional profile of each altitude in order to understand the whole structure of the wave development. In the case of 1998, strong stationary wave in July seen in

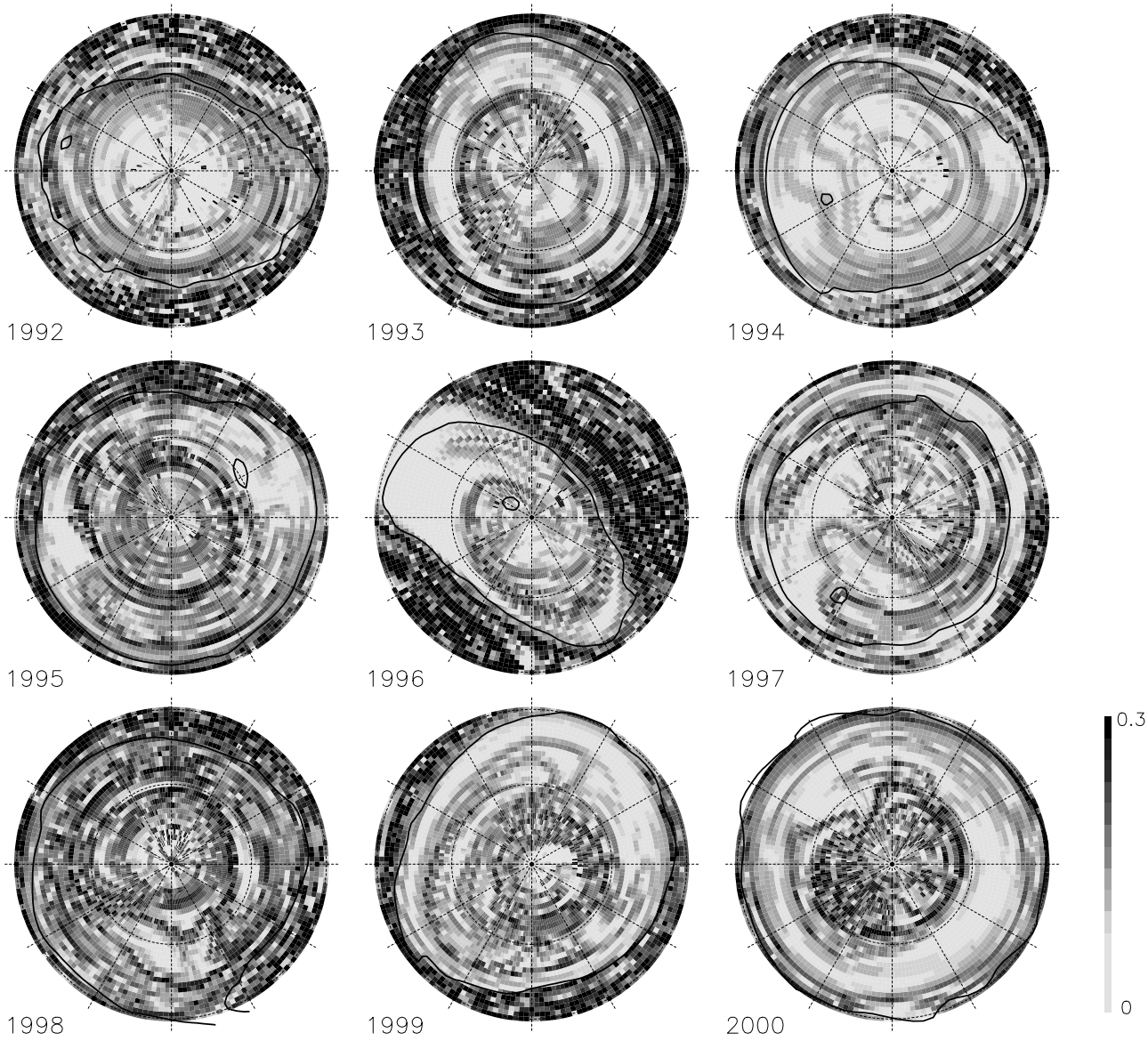

Figure 10. Distributions of the largest finite-time Lyapunov exponent (day^{-1}) on a 2° × 2° grid on the poleward side of 30°S. Evaluation time is 20 days.

Figure 1 might play an important role in the mixing process.

[27] Finite-time Lyapunov exponents shown in Figure 10, and the length of the advected contours in Figure 11 are used as linear and nonlinear measures of the strength of the mixing, respectively. Lyapunov exponents reflect the history of the linear deformation field that the trajectory experienced during the advection. Fine spatial structure can be found in the areas of high value. Since Lagrangian trajectory is sensitive to the initial position, growth of the distance of two nearby trajectories is also sensitive to the initial position. Therefore, the exponent calculated from a limited number of trajectories cannot represent the mixing of the region unless the evaluation time is long enough. On the other hand, contour advection can control the covered area and can examine larger area by one single contour. Material contours are often placed initially in concentric circles or isolines of PV in most of previous studies. Distortion and folding effect of the contours can be evaluated quantitatively, while small structures obtained by the finite-time Lyapunov exponents cannot be resolved. Effective diffusivity [*Nakamura*, 1996] is also useful for investigating meridional mixing in the equivalent latitude coordinate.

[28] Latitudes of strong mixing can be identified in the Lyapunov exponents (Figure 10). For example, the mixing is strong from 60°S to 80°S in 2000. The eastward propagating 4-day wave is seen in the same latitudes in the PV field (Figure 5), and is quasi-stationary with respect to the background flow since the wind speed in the polar region is close to a solid body rotation with the period of 3 or 4 days (Figure 3). Moreover, material lines are deformed with wave-breaking patterns in Figures 7 and 9. These features suggest that the region of strong signal of the 4-day wave corresponds to the critical latitude of the wave, and that air parcels are stirred and mixed in the critical layer. Counter gradient of the zonal mean flow field, the structure of the 4-

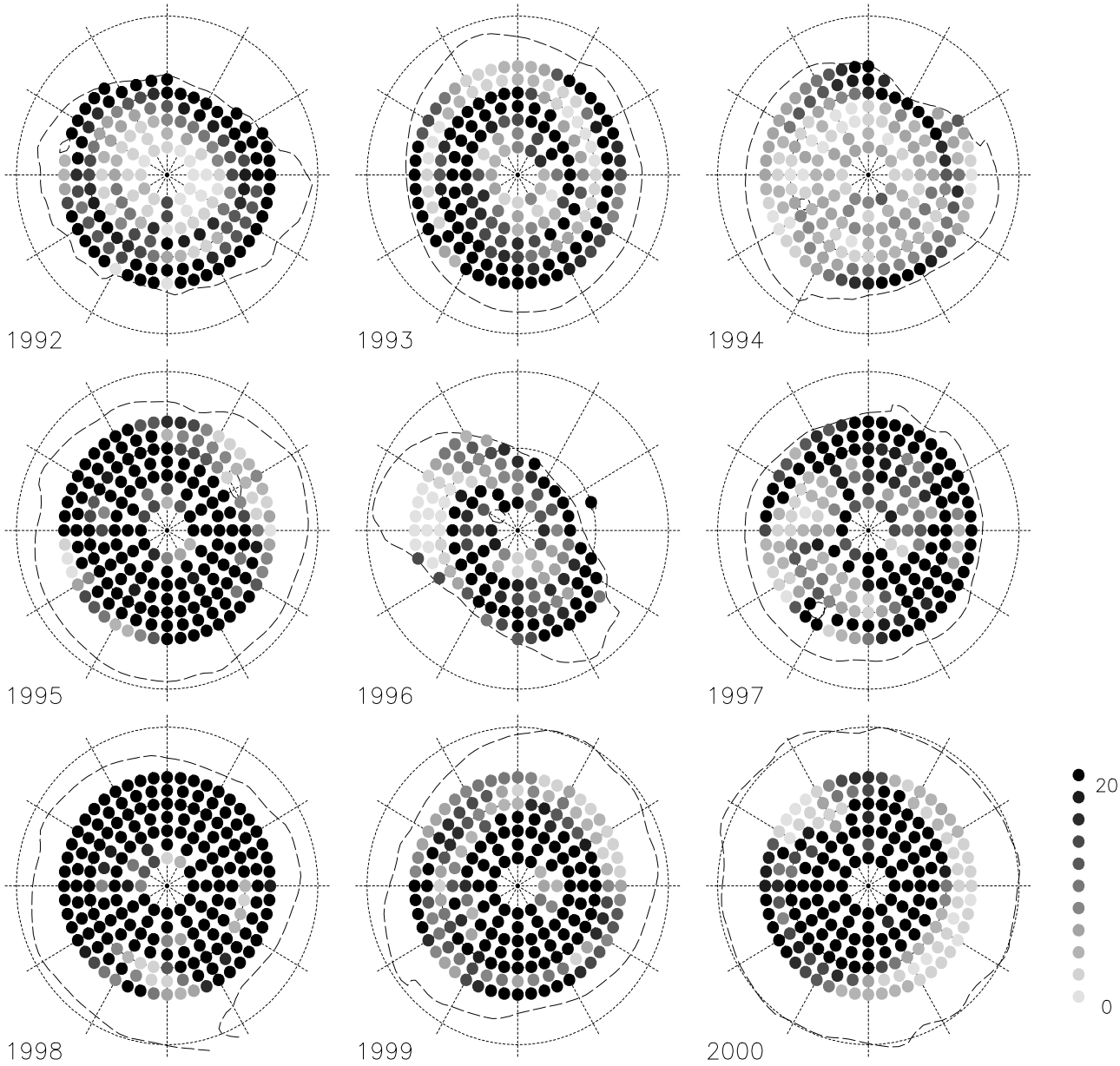

Figure 11. Grayscale map of the contour length after the 20-day advection since July 7. The material contours are put initially on the circumferences. The scale is relative to the initial length. Circles which existed outside the polar vortex at the initial time are not shown.

day wave, and enhancement of the horizontal mixing can be found on the lower levels down to 1150 K isentropic surface. However, they are not so evident as the results on 1800 K surface and it is difficult to relate to each other due to some other effects. The phenomenon that the mixing is strong only in a certain part of the polar vortex is also seen in the lower stratosphere. *Lee et al.* [2001] showed two distinct regions of a strongly mixed vortex core and a broad ring of weakly mixed air extending out to the vortex boundary.

6. Conclusions

[29] Zonal mean wind field in midwinter of the Southern Hemisphere upper stratosphere shows considerably large interannual variability in the nine years of 1992–2000. Activity of the eastward propagating 4-day wave in the polar region shows large interannual variability, although the amplitude is not very large without breakdown of the polar vortex. It is shown that large-scale horizontal stirring and mixing inside the polar vortex are highly correlated with the activity of the 4-day wave inside the polar vortex.

[30] When the wave has a large amplitude, effective mixing through stretching and folding process is seen inside the polar vortex. Finite-time Lyapunov exponents are sometimes as high as the midlatitudes, and the material contours of small areas grow exponentially in time. This effective mixing process is not uniform inside the vortex but limited to a part of the inside, and mixing is often seen on the poleward side of 70°S. When the wave is not clearly seen,

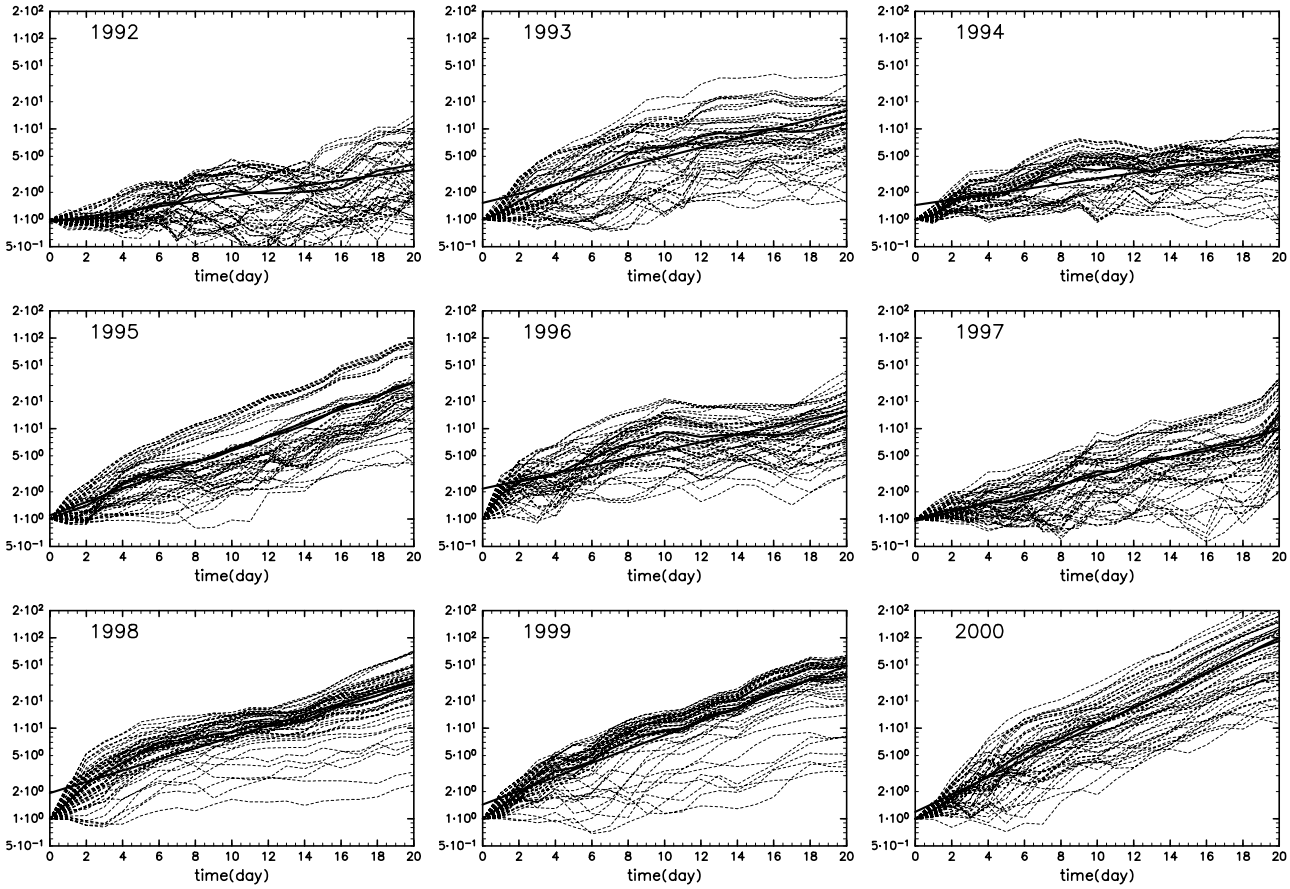

Figure 12. Time evolution of the contour length relative to the initial length. Contours initially put between 70°S and 80°S in Figure 11 are plotted in this figure. Thick lines are mean length of the contours. These are fitted to the thick straight lines.

on the other hand, wind fields are close to a solid body rotation around the pole and mixing is very small. The suppression of mixing is characterized by small Lyapunov exponents and linear growth of material contours, which are only stretched by the meridional shear on the poleward side of the polar night jet.

[31] Such interannual variability of the strength of the mixing inside the polar vortex is related to the interannual

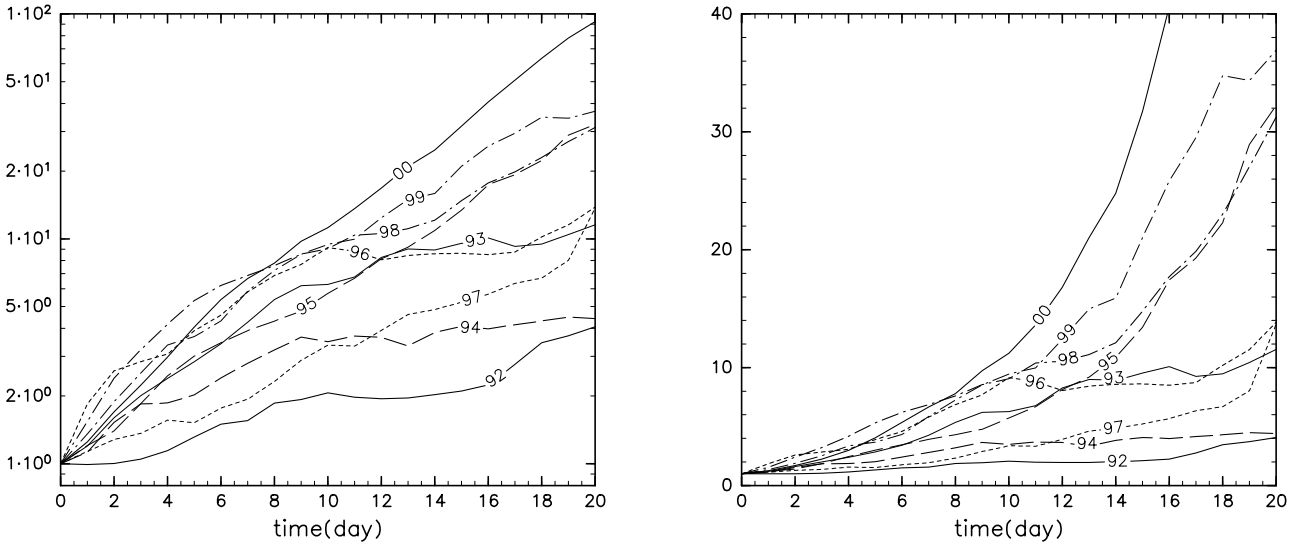

Figure 13. Time evolution of the mean contour length for each year of Figure 12 in a logarithm scale (left) and in a linear scale (right).

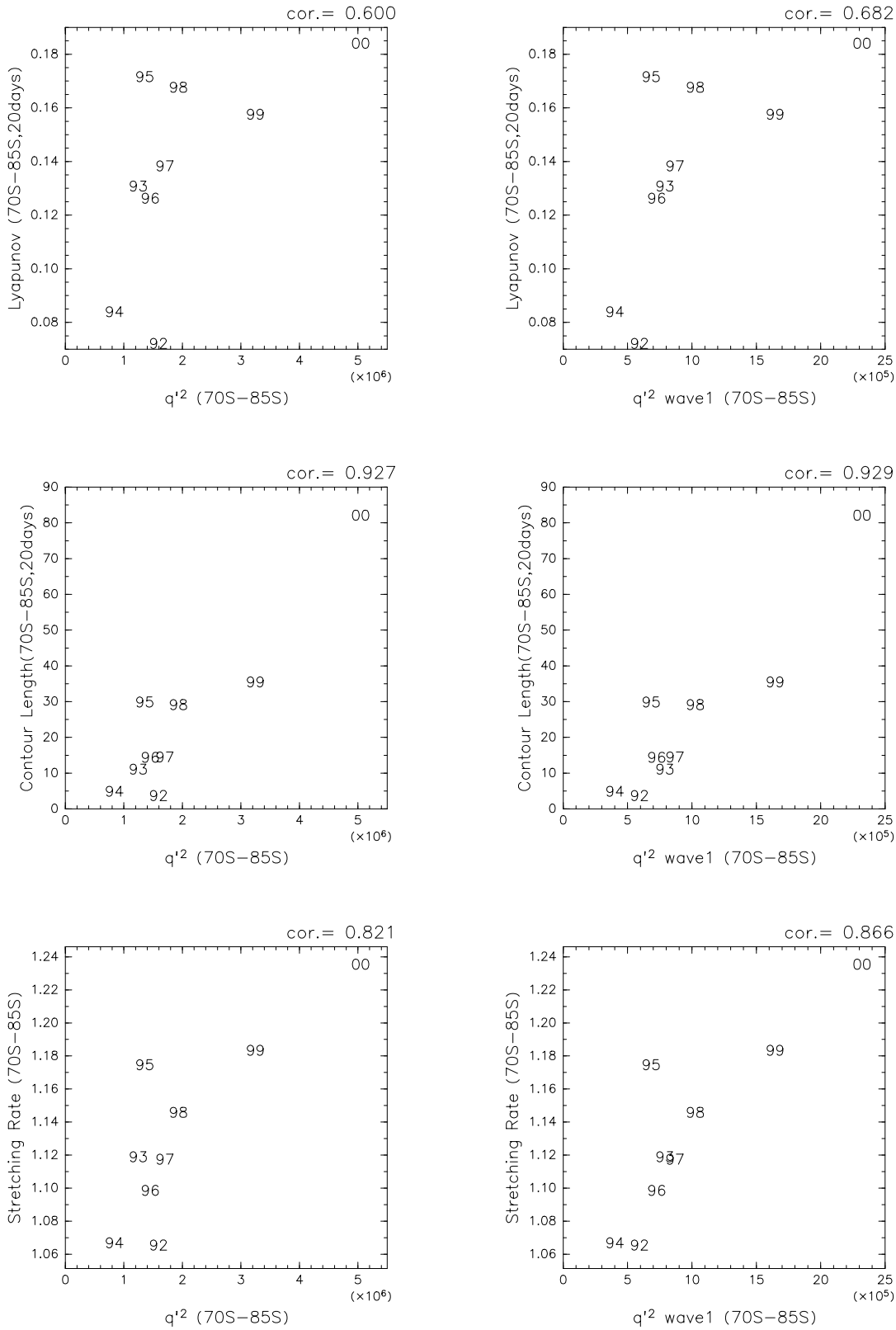

Figure 14. Relationships between the strength of the horizontal mixing and perturbation amplitude. Mean $\overline{q'^2}$ for 20 days between 70°S and 85°S (left), and average of wavenumber 1 component of that (right) is taken as the measure of the strength of disturbance. Three types of quantitative measure of the mixing are used: mean Lyapunov exponents between 70°S and 85°S in Figure 10 (top), mean contour length after the advection in Figure 11 (middle), and mean growth rate of the contour in Figure 12 (bottom). Numbers denote each year, and the correlation coefficient is also shown above each panel.

variability of the amplitude of the PV perturbation in that region. Above all, the mean stretching rate of the material contours is well correlated to the disturbance amplitude of zonal wavenumber 1 component. Although the 4-day wave is expected to be caused by the instability of the zonal mean zonal wind, the relationship between the mixing by the perturbation and the zonal mean fields is not always strong.

[32] **Acknowledgments.** We are grateful to U.K. Meteorological Office for providing the data sets and to Nozomi Kawamoto and Hiroo Hayashi for processing the data. This work has been supported by Grant-in-Aid for Scientific Research of the Ministry of Education, Culture, Sports, Science, and Technology of Japan. Computations were done at the Data Processing Center, Kyoto University. GFD-DENNOU Library (SGKS Group, DCL-5.2 (in Japanese), available online at http://www.gfd-dennou.org/library/dcl/, 2001) was used for drawing the figures.

References

Allen, D. R., and N. Nakamura, A seasonal climatology of effective diffusivity in the stratosphere, *J. Geophys. Res.*, *106*, 7917–7935, 2001.

Allen, D. R., J. L. Stanford, L. S. Elson, E. F. Fishbein, L. Froidevaux, and J. W. Waters, The 4-day wave as observed from the Upper Atmosphere Research Satellite Microwave Limb Sounder, *J. Atmos. Sci.*, *54*, 420–434, 1997.

Bowman, K. P., Large-scale isentropic mixing properties of the Antarctic polar vortex from analyzed winds, *J. Geophys. Res.*, *98*, 23,013–23,027, 1993.

Dritschel, D. G., Contour dynamics and contour surgery: Numerical algorithms for extended, high-resolution modeling of vortex dynamics in two-dimensional, inviscid, incompressible flows, *Comput. Phys. Rep.*, *10*, 77–146, 1989.

Hartmann, D. L., Barotropic instability of the polar night jet stream, *J. Atmos. Sci.*, *40*, 817–835, 1983.

Harwood, R. S., The temperature structure of the Southern Hemisphere stratosphere August–October 1971, *Q. J. R. Meteorol. Soc.*, *101*, 75–91, 1975.

Haynes, P. H., and E. F. Shuckburgh, Effective diffusivity as a diagnostic of atmospheric transport, 1, Stratosphere, *J. Geophys. Res.*, *105*, 22,777–22,794, 2000.

Holton, J. R., P. H. Haynes, M. E. McIntyre, A. R. Douglass, R. B. Rood, and L. Pfister, Stratosphere-troposphere exchange, *Rev. Geophys*, *33*, 403–439, 1995.

Hsu, H.-H., and S.-P. Weng, The stratospheric antarctic intraseasonal oscillation during the Austral winter, *J. Meteorol. Soc. Jpn.*, *80*, 1029–1050, 2002.

Lee, A. M., H. K. Roscoe, A. E. Jones, P. H. Haynes, E. F. Shuckburgh, M. W. Morrey, and H. C. Pumbhrey, The impact of the mixing properties within the Antarctic stratospheric vortex on ozone loss in spring, *J. Geophys. Res.*, *106*, 3203–3211, 2001.

Manney, G. L., and W. J. Randel, Instability at the winter stratopause: A mechanism for the 4-day wave, *J. Atmos. Sci.*, *50*, 3928–3938, 1993.

Manney, G. L., T. R. Nathan, and J. L. Stanford, Barotropic stability of realistic stratospheric jets, *J. Atmos. Sci.*, *45*, 2545–2555, 1988.

Manney, G. L., Y. J. Orsolini, H. C. Pumphrey, and A. E. Roche, The 4-day wave and transport of UARS tracers in the Austral polar vortex, *J. Atmos. Sci.*, *55*, 3456–3470, 1998.

Mizuta, R., and S. Yoden, Chaotic mixing and transport barriers in an idealized stratospheric polar vortex, *J. Atmos. Sci.*, *58*, 2616–2629, 2001.

Nakamura, N., Two-dimensional mixing, edge formation, and permeability diagnosed in area coordinates, *J. Atmos. Sci.*, *53*, 1524–1537, 1996.

Norton, W. A., Breaking Rossby waves in a model stratosphere diagnosed by a vortex-following coordinate system and a technique for advecting material contours, *J. Atmos. Sci.*, *51*, 654–673, 1994.

Pierce, R. B., T. D. Fairlie, W. L. Grose, R. Swinbank, and A. O'Neill, Mixing processes within the polar night jet, *J. Atmos. Sci.*, *51*, 2957–2972, 1994.

Plumb, R. A., Stratospheric transport, *J. Meteorol. Soc. Jpn.*, *80*, 793–809, 2002.

Plumb, R. A., et al., Intrusions into the lower stratospheric Arctic vortex during the winter of 1991–1992, *J. Geophys. Res.*, *99*, 1089–1105, 1994.

Schoeberl, M. R., L. R. Lait, P. A. Newman, and J. E. Rosenfield, The structure of the polar vortex, *J. Geophys. Res.*, *97*, 7859–7882, 1992.

Swinbank, R., and A. O'Neill, A stratosphere-troposphere data assimilation system, *Mon. Weather Rev.*, *122*, 686–702, 1994.

Venne, D. E., and J. L. Stanford, Observation of a 4-day temperature wave in the polar winter stratosphere, *J. Atmos. Sci.*, *36*, 2016–2019, 1979.

Waugh, D. W., and R. A. Plumb, Contour advection with surgery: A technique for investigating finescale structure in tracer transport, *J. Atmos. Sci.*, *51*, 530–540, 1994.

R. Mizuta and S. Yoden, Department of Geophysics, Kyoto University, Kyoto 606-8502, Japan. (mizuta@kugi.kyoto-u.ac.jp)